

Size-dependent deflection of cross-ply composite laminated plate induced by piezoelectric actuators based on a re-modified couple stress theory

H. WANG^{1,2)}, Z. LI³⁾, S. ZHENG^{1,*})

¹⁾State Key Laboratory of Mechanics and Control of Mechanical Structures, Nanjing University of Aeronautics and Astronautics, Nanjing 210016, PR China

²⁾College of Mechanical and Electrical Engineering, Nanjing University of Aeronautics and Astronautics, Nanjing, 210016, PR China

³⁾Pan Asia Technical Automotive Center Co. Ltd., Shanghai 2121, PR China, e-mail^{*)}: sjzheng@nuaa.edu.cn

A SIZE-DEPENDENT MODEL FOR CROSS-PLY COMPOSITE LAMINATED PLATE bonded with PZT actuators is developed by using re-modified couple stress theory (RMCST), which only uses two material length scale parameters to describe the size-dependent effect. An equivalent bending moment model and a refined model are developed by using two different ways. The analytical solution of equivalent bending moment model for simply supported composite laminated plate is obtained. The equilibrium equation of motion and corresponding boundary constraints of the refined model are established from the potential energy principle. The Ritz approximate solution of transverse deflection of the refined model indicates that the size-effect cannot be ignored in micro-scale. Numerical examples are given to account for the effect of material length scale parameters and dimensions of piezoelectric actuators on the deflection of composite laminated plate.

Key words: deflection, composite laminated plate, piezoelectric actuator, re-modified couple stress theory.

Copyright © 2019 by IPPT PAN, Warszawa

1. Introduction

THE PIEZOELECTRIC CERAMICS POSSESS THE ABILITIES of generating an electrical charge in response to an externally applied load and inducing mechanical strains in proportion of an electric potential. This kind of interaction between electrical and mechanical fields (named as direct and inverse piezoelectric effect) eventually has resulted in their extensive application as sensors and actuators in various engineering applications. When a very high electrical voltage results in only tiny variations in the width of crystal, the deformation should be controlled precisely in the range of micrometer. Thus piezoelectric crystals become the most

significant facility for positioning an object with greater accuracy. Piezoceramics are the most widely used piezoelectric crystals in smart structures and can be bonded to the composite plates or shells without remarkably altering the structural stiffness [1].

CRAWLEY and LUIS [2] established a model to predict the performance of flexible host-beams with segmented piezoelectric actuators. HUANG and SUN [3] presented the numerical development to analyze wave propagation in an anisotropic medium with surface-bonded piezoceramic actuators subject to high frequency electrical inputs. DIMITRIADIS *et al.* [4] studied the dynamic response of a simply supported elastic plate actuated by two dimensional patches of piezoelectric materials bonded to the surface of elastic structures. HER and LIN [1] developed a model to analyze the transverse deformation of a cross-ply composite laminated plate with a pair of symmetrically surface bonded piezoelectric actuators excited by equal-amplitude voltages with an opposite sign. LUO and TONG [5] used orthotropic PZT actuators to control the twisting and bending shapes for the specified plate of high precision. Other researches related to piezoelectric-based shape control of composite structures include LIN and NIEN [6] and BOWEN *et al.* [7, 8].

Piezoelectric components are also extensively used in micro-structures, such as micro-actuators [9], micro-sensors [10]. Numerous experiments have shown that size effects should be taken into consideration [11, 12] when microstructural size scales down to micrometers. Since the conventional continuum theory cannot account for this phenomenon because of the absence of internal material length scale parameters (IMLSP), many new theories for microstructures to capture the scale effect come into being. Among all these developed theories to explain this unusual experimental phenomenon, the most widely used theories include the classical couple stress theory [13, 14], the nonlocal elasticity theory [15] and the strain gradient theory [12]. Due to the difficulties of determining IMLSPs, aforementioned size-dependent theories are not very convenient to be used in practical application. Lately, since the pioneering work of YANG *et al.* [16] in which the couple stress tensor becomes symmetrical and the number of IMLSP is reduced to only one, the modified couple stress theory was widely used to analyze the size-dependent flexural deformation, free vibration and instability of micro-beams and micro-plates [17–24] as well as the pull-in phenomena in MEMS [25, 26].

A literature survey shows that the existing investigations primarily focus on the size-dependent functionally graded piezoelectric (FGP) beam and plate [27–30], piezoelectric microbeams [31] and piezoelectric nanobeam [32–34]. No work has been carried out on the investigation of size effect on piezoelectric laminated plates. So far, only a very few works [35–40] were reported for the piezoelectric laminated beam based on the modified couple stress theory (MCST). It is

worth noting that all of the aforementioned models are limited to an isotropic theory and are unable to solve anisotropic problems, especially establishing couple stress based laminated beam/plate models. Indeed, it is not straightforward to extend the couple stress theory [16] to establish composites laminated models. However, composite laminated materials have found increasing applications in engineering structures because of their high strength-to-weight and stiffness-to-weight ratios. Recently, CHEN *et al.* [41] have presented a re-modified couple stress theory to analyze the scale effects of anisotropy plate, such as the composite laminated Reddy plate, in which a new asymmetric curvature tensor is used to establish the constitutive relations of a laminated plate for anisotropy materials instead of the conventional symmetric one, and the former reduces to the latter in the case of isotropic elasticity. After this, CHEN and LI [42] established a size-dependent Timoshenko beam model to study the free vibration of composite laminated beam by using RMCST. Chen and his collaborator also developed a size-dependent composite laminated plate model by using the global-local theory [43]. MOHAMMADABADI *et al.* [44] used this theory to investigate the effect of temperature on size-dependent buckling of a composite laminated micro-beam. To the best of authors' knowledge, however, size-dependent investigation of composite laminated piezoelectric plate based on RMCST for orthotropic anisotropy materials [41, 45] has not been presented so far. At present, micro- and nano-scale composite beams and/or plates are generally utilized in micro/nano- electromechanical systems (MEMS/ NEMS), such as resonant microsensors [46], micro-pumps [47], micro-switches [48], micro-mirrors [49] as well as Atomic Force Microscope [50] and so on. Among them, thin composite micro-plates with a piezoelectric layer have many applications. For example, many investigators pointed out that piezoelectric micro/nano-structures can be utilized to enhance the property of resonant microsensors acting as signal filtering and chemical and mass sensing [51]. As another example, a piezoelectric actuator also plays the role of actuating a composite micro-plate in an atomic force microscopes for topography and manipulation operation [50]. To promote these wishing applications, the increasing understanding of the mechanical behaviors of foregoing piezoelectric micro/nano-plates is becoming more and more important. This motivates our present research.

This paper presents a size-dependent analysis of the transverse deformation of a cross-ply composite laminated plate excited by piezoelectric actuators by using RMCST. The present model only has two IMLSPs to account for the scale effect. Equal-amplitude voltages with an opposite sign are applied to the two PZT actuators. An equivalent bending moment model and a refined model are developed by two different ways. The analytical solution of the equivalent bending moment model for simply supported composite laminated plate is obtained. The equilibrium equation and corresponding boundary conditions of the refined

model are obtained from the potential energy principle. The Ritz approximate solution of deflection of the refined model indicates that the size-effect cannot be ignored in micro-scale. Numerical examples are introduced to account for the effect of IMLSPs and dimensions of piezoelectric actuators on the deflection of composite laminated plate.

2. Modified couple stress theory

According to MCST [16] for isotropic linear elasticity, the virtual strain energy of a deformed body occupying the region Ω is given as:

$$(2.1) \quad \delta U = \int_{\Omega} (\sigma_{ij} \delta \varepsilon_{ij} + m_{ij} \delta \chi_{ij}) d\Omega,$$

where repeated indices imply summation; σ_{ij} and ε_{ij} denote the stress tensors and the strain tensors, respectively; m_{ij} and χ_{ij} are the couple stress tensors and the symmetric curvature tensors, respectively. The strain tensors, symmetric curvature tensors are defined as follows:

$$(2.2) \quad \begin{cases} \varepsilon_{ij} = \frac{1}{2}(u_{i,j} + u_{j,i}), \\ \chi_{ij} = \frac{1}{2}(\omega_{i,j} + \omega_{j,i}), \end{cases}$$

where u_i is the component of the displacement vector and ω_i represents the infinitesimal rotation tensor; ε_{ij} and χ_{ij} are symmetric tensor, and $\boldsymbol{\omega} = \text{curl}(\mathbf{u})/2$.

Using the curvature and strain tensors, the constitutive relations can be given as:

$$(2.3) \quad \begin{cases} \sigma_{ij} = \lambda \varepsilon_{kk} \delta_{ij} + 2G \varepsilon_{ij}, \\ m_{ij} = 2Gl^2 \chi_{ij}, \end{cases}$$

where l is the material length scale parameter; λ and G are elasticity constants, and δ_{ij} is the Kronecker delta.

3. RMSCT for composite laminated plate

A new constitutive equation between couple stress and curvatures for the k th ply can be written as [41]:

$$(3.1) \quad \begin{Bmatrix} m_{x'} \\ m_{y'} \\ m_{x'y'} \\ m_{y'x'} \end{Bmatrix} = \begin{bmatrix} 2l_{kb}^2 C_{44}^k & & & \\ & 2l_{km}^2 C_{55}^k & & \\ & & l_{kb}^2 C_{44}^k & l_{km}^2 C_{55}^k \\ & & l_{kb}^2 C_{44}^k & l_{km}^2 C_{55}^k \end{bmatrix} \begin{Bmatrix} \frac{\partial \omega_{x'}}{\partial x'} \\ \frac{\partial \omega_{y'}}{\partial y'} \\ \frac{\partial \omega_{x'}}{\partial y'} \\ \frac{\partial \omega_{y'}}{\partial x'} \end{Bmatrix},$$

$$(3.12) \quad \begin{cases} l^2 \tilde{Q}_{44}^k = l_{kb}^2 C_{44}^k m^4 + l_{km}^2 C_{55}^k n^4 + 4m^2 n^4 (l_{kb}^2 C_{44}^k + l_{km}^2 C_{55}^k), \\ l^2 \tilde{Q}_{45}^k = -3m^2 n^4 (l_{kb}^2 C_{44}^k + l_{km}^2 C_{55}^k), \\ l^2 \tilde{Q}_{55}^k = l_{kb}^2 C_{44}^k n^4 + l_{km}^2 C_{55}^k m^4 + 4m^2 n^2 (l_{kb}^2 C_{44}^k + l_{km}^2 C_{55}^k), \\ l^2 \tilde{Q}_{46}^k = mn(m^2 l_{kb}^2 C_{44}^k - n^2 l_{km}^2 C_{55}^k), \\ l^2 \tilde{Q}_{47}^k = -mn(m^2 + 2n^2) l_{kb}^2 C_{44}^k + mn(n^2 + 2m^2) l_{km}^2 C_{55}^k, \\ l^2 \tilde{Q}_{56}^k = -mn(n^2 + 2m^2) l_{kb}^2 C_{44}^k + mn(m^2 + 2n^2) l_{km}^2 C_{55}^k, \\ l^2 \tilde{Q}_{57}^k = mn(n^2 l_{kb}^2 C_{44}^k - m^2 l_{km}^2 C_{55}^k), \\ l^2 \hat{Q}_{44}^k = l_{kb}^2 C_{44}^k m^4 + l_{km}^2 C_{55}^k n^4 + m^2 n^4 (l_{kb}^2 C_{44}^k + l_{km}^2 C_{55}^k), \\ l^2 \hat{Q}_{55}^k = l_{kb}^2 C_{44}^k n^4 + l_{km}^2 C_{55}^k m^4 + m^2 n^2 (l_{kb}^2 C_{44}^k + l_{km}^2 C_{55}^k). \end{cases}$$

4. Equations of composite laminated plate induced by PZT actuators based on the new RMCST

Two piezoelectric actuators are symmetrically bonded to the surface of a cross-ply composite laminated plate, as shown in Fig. 1. Two identical piezoelectric elements are driven 180° out of phase with the same signals. As an electrical voltage is acted along the direction of polarization, the induced actuators cause the composite laminated plate to bend. For a free thin PZT patch, the magnitude of the induced strains can be written as follows:

$$(4.1) \quad (\varepsilon_x)_{pe} = (\varepsilon_y)_{pe} = \varepsilon_{pe} = \frac{d_{31}}{t_{pe}} V,$$

where d_{31} , t_{pe} and V are the piezoelectric constant, actuator thickness and applied voltage, respectively.

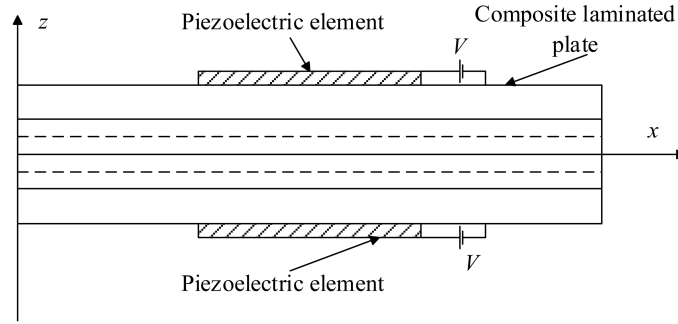


FIG. 1. Schematic diagram of composite laminated plate and piezoelectric actuators.

According to the Kirchhoff plate theory, the displacement field of composite laminated plate can be written as:

$$(4.2) \quad u = -z \frac{\partial w}{\partial x}, \quad v = -z \frac{\partial w}{\partial y}, \quad w = w(x, y).$$

For piezoelectric actuators, the stress in the top piezoelectric element is given by:

$$\begin{aligned}
 (\sigma_x^1)_{pe} &= \frac{E_{pe}}{1 - \nu_{pe}^2} (\varepsilon_x + \nu_{pe} \varepsilon_y - (1 + \nu_{pe}) \varepsilon_{pe}), \\
 (\sigma_y^1)_{pe} &= \frac{E_{pe}}{1 - \nu_{pe}^2} (\nu_{pe} \varepsilon_x + \varepsilon_y - (1 + \nu_{pe}) \varepsilon_{pe}), \\
 (\sigma_{xy}^1)_{pe} &= \frac{E_{pe}}{1 - \nu_{pe}^2} \gamma_{xy}, \\
 (m_x^1)_{pe} &= 2G_{pe} l_{pe}^2 (\chi_x)_{pe}, \\
 (m_y^1)_{pe} &= 2G_{pe} l_{pe}^2 (\chi_y)_{pe}, \\
 (m_{xy}^1)_{pe} &= 2G_{pe} l_{pe}^2 (\chi_{xy})_{pe}.
 \end{aligned}
 \tag{4.9}$$

For the bottom piezoelectric layer, the stress can be expressed as:

$$\begin{aligned}
 (\sigma_x^2)_{pe} &= \frac{E_{pe}}{1 - \nu_{pe}^2} (\varepsilon_x + \nu_{pe} \varepsilon_y + (1 + \nu_{pe}) \varepsilon_{pe}), \\
 (\sigma_y^2)_{pe} &= \frac{E_{pe}}{1 - \nu_{pe}^2} (\nu_{pe} \varepsilon_x + \varepsilon_y + (1 + \nu_{pe}) \varepsilon_{pe}), \\
 (\sigma_{xy}^2)_{pe} &= \frac{E_{pe}}{1 - \nu_{pe}^2} \gamma_{xy}, \\
 (m_x^2)_{pe} &= 2G_{pe} l_{pe}^2 (\chi_x)_{pe}, \\
 (m_y^2)_{pe} &= 2G_{pe} l_{pe}^2 (\chi_y)_{pe}, \\
 (m_{xy}^2)_{pe} &= 2G_{pe} l_{pe}^2 (\chi_{xy})_{pe},
 \end{aligned}
 \tag{4.10}$$

where the subscript ‘ pe ’ denotes the piezoelectric element l_{pe} is the material length scale parameter, E_{pe} is the Young’s modulus, G_{pe} and ν_{pe} represent the shear modulus and Poisson’s ratio, respectively. The curvature tensor can be written as:

$$\begin{cases}
 (\chi_x)_{pe} = \frac{\partial^2 w}{\partial x \partial y}, \\
 (\chi_y)_{pe} = -\frac{\partial^2 w}{\partial x \partial y}, \\
 (\chi_{xy})_{pe} = \frac{1}{2} \left(\frac{\partial^2 w}{\partial y^2} - \frac{\partial^2 w}{\partial x^2} \right).
 \end{cases}
 \tag{4.11}$$

5. The model of equivalent bending moment

Applying the moment equilibrium equation with respect to y -axis i.e. (the neutral axis, shown in Fig. 1), yields

$$\begin{aligned}
& \int_{-h/2}^{h/2} m_x^k dZ + \int_{-h/2}^{h/2} \sigma_x^k Z dZ + \int_{-h/2-t_{pe}}^{-h/2} (\sigma_x^2)_{pe} Z dZ \\
& + \int_{h/2}^h (\sigma_x^1)_{pe} Z dZ + \int_{h/2}^{h/2+t_{pe}} (m_x^1)_{pe} dZ + \int_{-h/2-t_{pe}}^{-h/2} (m_x^2)_{pe} dZ = 0, \\
(5.1) \quad & \int_{-h/2}^{h/2} m_y^k dZ + \int_{-h/2}^{h/2} \sigma_y^k Z dZ + \int_{-h/2-t_{pe}}^{-h/2} (\sigma_y^2)_{pe} Z dZ + \int_{h/2}^{h/2+t_{pe}} (\sigma_y^1)_{pe} Z dZ \\
& + \int_{h/2}^{h/2+t_{pe}} (m_y^1)_{pe} dZ + \int_{-h/2-t_{pe}}^{-h/2} (m_y^2)_{pe} dZ = 0, \\
& \int_{-h/2}^{h/2} m_{xy}^k dZ + \int_{-h/2}^{h/2} m_{yx}^k dZ + \int_{-h/2}^{h/2} (\sigma_{xy}^k)_p Z dZ + \int_{-h/2-t_{pe}}^{-h/2} (\sigma_{xy}^2)_{pe} Z dZ \\
& + \int_{h/2}^{h/2+t_{pe}} (\sigma_{xy}^1)_{pe} Z dZ + \int_{h/2}^{h/2+t_{pe}} (m_{xy}^1)_{pe} dZ + \int_{-h/2-t_{pe}}^{-h/2} (m_{xy}^2)_{pe} dZ = 0,
\end{aligned}$$

where h and t_{pe} denote the thickness of the composite laminated plate and the thickness of piezoelectric actuators, respectively.

Substituting Eqs. (4.6), (4.9) and (4.10) into Eq. (5.1), we obtain:

$$\begin{aligned}
(5.2) \quad & [\bar{I}_{11} + 2(D_{11})_{pe}] \kappa_x + [\bar{I}_{12} + 2(D_{12})_{pe}] \kappa_y + [2l^2 \tilde{Q}_{44}^+ l_{pe}^2 (Y_{pe})] \kappa_{xy} \\
& = (1 + \nu_{pe}) 2(B_{11})_{pe} \varepsilon_{pe}, \\
& [\bar{I}_{12} + 2(D_{12})_{pe}] \kappa_x + [\bar{I}_{22} + 2(D_{22})_{pe}] \kappa_y + [-2l^2 \tilde{Q}_{55}^- 4l_{pe}^2 (Y_{pe})] \kappa_{xy} \\
& = (1 + \nu_{pe}) 2(B_{11})_{pe} \varepsilon_{pe}, \\
& [-l^2 \tilde{Q}_{55}^- - l_{pe}^2 (Y_{pe})] \kappa_x + [l^2 \tilde{Q}_{44} + l_{pe}^2 (Y_{pe})] \kappa_y + [2(D_{11})_{pe} + \bar{I}_{66}] \kappa_{xy} = 0,
\end{aligned}$$

where

$$\begin{aligned}
(5.3) \quad & \kappa_x = \frac{\partial^2 w}{\partial x^2}, \\
& \kappa_y = \frac{\partial^2 w}{\partial y^2}, \\
& \kappa_{xy} = \frac{\partial^2 w}{\partial x \partial y}
\end{aligned}$$

and

$$\begin{aligned}
 \bar{I}_{ij} &= \sum_{k=1}^n \frac{Q_{ij}^k (z_{k+1}^3 - z_k^3)}{3} \\
 I^2 \tilde{Q}_{ij} &= \sum_{k=1}^n [l_{kb}^2 \tilde{Q}_{ij}^k (z_{k+1} - z_k)] \\
 (Y)_{pe} &= G_{pe} t_{pe}, \\
 (B_{11})_{pe} &= \frac{1}{2} \frac{E_{pe}}{1 - \nu_{pe}^2} ((t_{pe} + h/2)^2 - (h/2)^2), \\
 (D_{12})_{pe} &= \frac{1}{3} \frac{\nu_{pe} E_{pe}}{1 - \nu_{pe}^2} ((t_{pe} + h/2)^3 - (h/2)^3), \\
 (D_{11})_{pe} &= (D_{22})_{pe} = \frac{1}{3} \frac{E_{pe}}{1 - \nu_{pe}^2} ((t_{pe} + h/2)^3 - (h/2)^3),
 \end{aligned}
 \tag{5.4}$$

where Z_k denotes the position of the upper surface of the k th layer in the composite laminated plate Z_{k-1} the lower surface

From Eq. (5.2), κ_x , κ_y and κ_{xy} can be expressed as:

$$(5.5) \quad \kappa_x = A_1 \varepsilon_{pe}, \quad \kappa_y = A_2 \varepsilon_{pe}, \quad \kappa_{xy} = A_3 \varepsilon_{pe},$$

where A_1 , A_2 and A_3 are the unknown algebraic formula obtained by solving Eq. (5.2)

The moment induced by a piezoelectric actuator in both x and y directions per unit length can be calculated:

$$\begin{aligned}
 M_x^{pe} &= \sum_{k=1}^N \left[\int_{Z_{k-1}}^{Z_k} Z \sigma_x^k dz \right] + \sum_{k=1}^N \left[\int_{Z_{k-1}}^{Z_k} m_x^k dz \right] \\
 &= \sum_{k=1}^N \left[\int_{Z_{k-1}}^{Z_k} Z^2 (Q_{11}^k \kappa_x + Q_{12}^k \kappa_y) dz \right] + \sum_{k=1}^N \left[\int_{Z_{k-1}}^{Z_k} 2l^2 \tilde{Q}_{44}^k \kappa_{xy} dz \right], \\
 M_y^{pe} &= \sum_{k=1}^N \left[\int_{Z_{k-1}}^{Z_k} Z \sigma_y^k dz \right] + \sum_{k=1}^N \left[\int_{Z_{k-1}}^{Z_k} m_y^k dz \right] \\
 &= \sum_{k=1}^N \left[\int_{Z_{k-1}}^{Z_k} Z^2 (Q_{12}^k \kappa_x + Q_{22}^k \kappa_y) dz \right] - \sum_{k=1}^N \left[\int_{Z_{k-1}}^{Z_k} 2l^2 \tilde{Q}_{55}^k \kappa_{xy} dz \right].
 \end{aligned}
 \tag{5.6}$$

The substitution of Eq. (5.5) into Eq. (5.6) permits this term to be reformulated as:

$$(5.7) \quad \begin{aligned} M_x^{pe} &= C_1 \varepsilon_{pe}, \\ M_y^{pe} &= C_2 \varepsilon_{pe}, \end{aligned}$$

where

$$(5.8) \quad \begin{aligned} C_1 &= (\bar{I}_{11}A_1 + \bar{I}_{12}A_2 + 2l^2\tilde{Q}_{44}A_3), \\ C_2 &= (\bar{I}_{12}A_1 + \bar{I}_{22}A_2 - 2l^2\tilde{Q}_{55}A_3). \end{aligned}$$

The induced moment by the piezoelectric actuators can also be expressed as:

$$(5.9) \quad \begin{aligned} M_x^{pe} &= C_1 \varepsilon_{pe} [H(x - x_1) - H(x - x_2)][H(y - y_1) - H(y - y_2)], \\ M_y^{pe} &= C_2 \varepsilon_{pe} [H(x - x_1) - H(x - x_2)][H(y - y_1) - H(y - y_2)], \end{aligned}$$

where (x_1, y_1) and (x_2, y_2) are the coordinates of the actuator corners as depicted in Fig. 2. $H(x)$ is the unit Heaviside step function defined as:

$$(5.10) \quad H(x) = \begin{cases} 1, & x > 0, \\ 0, & x < 0. \end{cases}$$

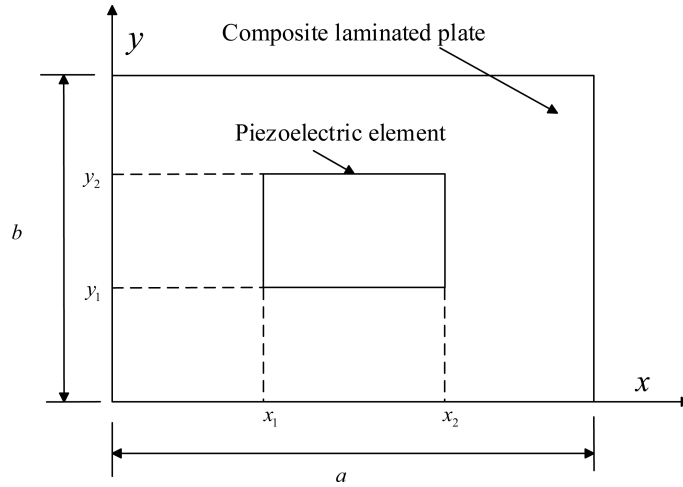


FIG. 2. The coordinates of the piezoelectric actuator.

The equilibrium equation for the composite laminated plate is given by:

$$(5.11) \quad \begin{aligned} (\bar{I}_{11} + l^2\tilde{Q}_{55}) \frac{\partial^4 w}{\partial x^4} + (2\bar{I}_{12} + 4\bar{I}_{66} + l^2\tilde{Q}_{44} + l^2\tilde{Q}_{55}) \frac{\partial^4 w}{\partial x^2 \partial y^2} \\ + (\bar{I}_{22} + l^2\tilde{Q}_{44}) \frac{\partial^4 w}{\partial y^4} = P, \end{aligned}$$

where

$$(5.12) \quad P = \frac{\partial^2 M_x^{pe}}{\partial x^2} + \frac{\partial^2 M_y^{pe}}{\partial y^2}.$$

The substitution of Eqs. (5.9) and (5.12) into (5.11), permits this term to be reexpressed as:

$$(5.13) \quad \begin{aligned} & (\bar{I}_{11} + l^2 \tilde{Q}_{55}) \frac{\partial^4 w}{\partial x^4} + (2\bar{I}_{12} + 4\bar{I}_{66} + l^2 \tilde{Q}_{44} + l^2 \tilde{Q}_{55}) \frac{\partial^4 w}{\partial x^2 \partial y^2} \\ & + (\bar{I}_{22} + l^2 \tilde{Q}_{44}) \frac{\partial^4 w}{\partial y^4} \\ & = C_1 \varepsilon_{pe} [\delta'(x - x_1) - \delta'(x - x_2)] [H(y - y_1) - H(y - y_2)] \\ & + C_2 \varepsilon_{pe} [H(x - x_1) - H(x - x_2)] [\delta'(y - y_1) - \delta'(y - y_2)], \end{aligned}$$

where $\delta'(\cdot)$ denotes the partial derivative of the Dirac delta function with respect to its argument.

By using a Fourier series, the transverse deflection of a simply supported rectangular plate can be expanded as:

$$(5.14) \quad w(x, y) = \sum_{m=1}^{\infty} \sum_{n=1}^{\infty} W_{mn} \sin \frac{m\pi x}{a} \sin \frac{n\pi y}{b}.$$

Substituting Eq. (5.14) into Eq. (5.13), the unknown constants to be determined can be expressed as:

$$(5.15) \quad W_{mn} = \frac{P_{mn}}{\frac{m^4 \pi^4}{a^4} (\bar{I}_{11} + l^2 \tilde{Q}_{55}) + \frac{m^2 \pi^2}{a^2} \frac{n^2 \pi^2}{b^2} (2\bar{I}_{12} + 4\bar{I}_{66} + l^2 \tilde{Q}_{44} + l^2 \tilde{Q}_{55}) + \frac{n^4 \pi^4}{b^4} (\bar{I}_{22} + l^2 \tilde{Q}_{44})},$$

where

$$(5.16) \quad \begin{aligned} P_{mn} &= \frac{4}{a*b} \int_0^b \int_0^a P(x, y) \sin \frac{m\pi x}{a} \sin \frac{n\pi y}{b} dx dy \\ &= \frac{4\varepsilon_{pe}}{a*b} \left[-\frac{C_2 \beta_m^2 + C_1 \alpha_n^2}{\beta_m \alpha_n} (\cos \beta_m x_1 - \cos \beta_m x_2) (\cos \alpha_n y_1 - \cos \alpha_n y_2) \right], \\ \beta_m &= \frac{m\pi}{a}, \quad \alpha_n = \frac{n\pi}{b}. \end{aligned}$$

As a special case, the present model degenerates to the model proposed by HER and LIN [1] when the size effect is ignored ($l = 0$).

6. A refined model developed by the potential energy principle

The model proposed in Section 5 is only suitable for the lesser actuator thickness. This section presents a refined model, whose solution strictly satisfies the partial differential control equations and associated boundary conditions of a composite laminated plate bonded with piezoelectric actuators. The potential energy principle for composite laminated plate and piezoelectric elements is given by:

$$(6.1) \quad \delta U - \delta W = 0,$$

where U and W denote the strain energy of the flexible body and the work done by the external forces, respectively. In the present model, no external force is produced ($W = 0$). The first variation of strain energy is expressed as:

$$(6.2) \quad \delta U = \delta U_c + \delta U_p,$$

where

$$(6.3) \quad \begin{aligned} \delta U_c &= \sum_{k=1}^n \delta U^k = \sum_{k=1}^n \int_{V^k} (\sigma_m^k \delta \varepsilon_m + m^k \delta \chi) dx dy dz \\ &= \int_{\Omega} \left(\sum_{k=1}^n \int_{z_k}^{z_{k+1}} (\sigma_x^k \delta \varepsilon_x + \sigma_y^k \delta \varepsilon_y + \sigma_{xy}^k \delta \gamma_{xy} + m_x^k \delta \chi_x + m_y^k \delta \chi_y \right. \\ &\quad \left. + m_{xy}^k \delta \chi_{xy} + m_{yx}^k \delta \chi_{yx}) dz \right) d\Omega \\ &= \int_{\Omega} \left((-M_{cx} - Y_{cyy}) \frac{\partial^2 \delta w}{\partial x^2} + (-M_{cy} + Y_{cxy}) \frac{\partial^2 \delta w}{\partial y^2} \right. \\ &\quad \left. + (-2M_{cxy} + Y_{cx} - Y_{cy}) \frac{\partial^2 \delta w}{\partial x \partial y} \right) d\Omega, \end{aligned}$$

$$(6.4) \quad \begin{aligned} \delta U_p &= \int_A \int_h^{h+t_{pe}} (\sigma_{xx} \delta \varepsilon_x + \sigma_{yy} \delta \varepsilon_y + \sigma_{xy} \delta \gamma_{xy} \\ &\quad + m_x \delta \chi_x + m_y \delta \chi_y + 2m_{xy} \delta \chi_{xy}) dAdz \\ &\quad + \int_A \int_{-h-t_{pe}}^{-h} (\sigma_{xx} \delta \varepsilon_x + \sigma_{yy} \delta \varepsilon_y + \sigma_{xy} \delta \gamma_{xy} \\ &\quad + m_x \delta \chi_x + m_y \delta \chi_y + 2m_{xy} \delta \chi_{xy}) dAdz \\ &= \int_A \left((\bar{M}_{xx} + 2E_p) \frac{\partial^2 \delta w}{\partial x^2} + (\bar{M}_{yy} + 2E_p) \frac{\partial^2 \delta w}{\partial y^2} + \bar{M}_{xy} \frac{\partial^2 \delta w}{\partial x \partial y} \right) dA, \end{aligned}$$

where

$$\begin{aligned}
 \bar{M}_{xx} &= -M_{pex}^1 - Y_{pexy}^1 - M_{pex}^2 - Y_{pexy}^2, \\
 \bar{M}_{yy} &= -M_{pey}^1 + Y_{pexy}^1 - M_{pey}^2 + Y_{pexy}^2, \\
 \bar{M}_{xy} &= -2M_{pexy}^1 + Y_{pex}^1 - Y_{pey}^1 - 2M_{pexy}^2 + Y_{pex}^2 - Y_{pey}^2, \\
 (6.5) \quad (M_{cx}, M_{cy}, M_{cxy}) &= \sum_{k=1}^n \int_{z_k}^{z_{k+1}} (\sigma_x^k, \sigma_y^k, \sigma_{xy}^k) z dz, \\
 (Y_{cx}, Y_{cy}, Y_{cxy}, Y_{cyx}) &= \sum_{k=1}^n \int_{z_k}^{z_{k+1}} (m_x^k, m_y^k, m_{xy}^k, m_{yx}^k) dz, \\
 (M_{pex}^1, M_{pey}^1, M_{pexy}^1) &= \int_{h/2}^{h/2+t_{pe}} ((\sigma_x^1)_{pe}, (\sigma_y^1)_{pe}, (\sigma_{xy}^1)_{pe}) z dz, \\
 (Y_{pex}^1, Y_{pey}^1, Y_{pexy}^1) &= \int_{h/2}^{h/2+t_{pe}} ((m_x^1)_{pe}, (m_y^1)_{pe}, (m_{xy}^1)_{pe}) dz, \\
 (M_{pex}^2, M_{pey}^2, M_{pexy}^2) &= \int_{-h/2-t_{pe}}^{-h/2} ((\sigma_x^2)_{pe}, (\sigma_y^2)_{pe}, (\sigma_{xy}^2)_{pe}) z dz, \\
 (Y_{pex}^2, Y_{pey}^2, Y_{pexy}^2) &= \int_{-h/2-t_{pe}}^{-h/2} ((m_x^2)_{pe}, (m_y^2)_{pe}, (m_{xy}^2)_{pe}) dz.
 \end{aligned}$$

Substituting Eqs.(4.5)–(4.7) and Eqs. (4.9)–(4.11) into (6.5), we can obtain

$$\begin{aligned}
 M_{cx} &= -\bar{I}_{11} \frac{\partial^2 w}{\partial x^2} - \bar{I}_{12} \frac{\partial^2 w}{\partial y^2}, \\
 M_{cy} &= -\bar{I}_{12} \frac{\partial^2 w}{\partial x^2} - \bar{I}_{22} \frac{\partial^2 w}{\partial y^2}, \quad M_{cxy} = -2\bar{I}_{66} \frac{\partial^2 w}{\partial x \partial y}, \\
 Y_{cx} &= 2l^2 \tilde{Q}_{44} \frac{\partial^2 w}{\partial x \partial y}, \\
 Y_{cy} &= -2l^2 \tilde{Q}_{55} \frac{\partial^2 w}{\partial x \partial y}, \\
 Y_{cxy} &= Y_{cyx} = l^2 \tilde{Q}_{44} \frac{\partial^2 w}{\partial y^2} - l^2 \tilde{Q}_{55} \frac{\partial^2 w}{\partial x^2},
 \end{aligned}$$

$$\begin{aligned}
(6.6) \quad M_{pex}^1 &= M_{pex}^2 = -C_{11}^{12} \frac{\partial^2 w}{\partial x^2} - C_{12}^{12} \frac{\partial^2 w}{\partial y^2}, \\
M_{pey}^1 &= M_{pey}^2 = -C_{12}^{12} \frac{\partial^2 w}{\partial x^2} - C_{11}^{12} \frac{\partial^2 w}{\partial y^2}, \\
M_{pexy}^1 &= M_{pexy}^2 = -2C_{11}^{12} \frac{\partial^2 w}{\partial x \partial y}, \\
Y_{pex}^1 &= Y_{pex}^2 = \mathbb{G}_{pe} \frac{\partial^2 w}{\partial x \partial y}, \\
Y_{pey}^1 &= Y_{pey}^2 = -\mathbb{G}_{pe} \frac{\partial^2 w}{\partial x \partial y}, \\
Y_{pexy}^1 &= Y_{pexy}^2 = \frac{1}{2} \mathbb{G}_{pe} \left(\frac{\partial^2 w}{\partial y^2} - \frac{\partial^2 w}{\partial x^2} \right),
\end{aligned}$$

where

$$\begin{aligned}
(6.7) \quad C_{11}^{12} &= \int_{h/2}^{h/2+t_{pe}} \frac{E_{pe}}{1-v_{pe}^2} z^2 dz = \int_{-h/2-t_{pe}}^{-h/2} \frac{E_{pe}}{1-v_{pe}^2} z^2 dz, \\
C_{12}^{12} &= \int_{h/2}^{h/2+t_{pe}} \frac{v_{pe} E_{pe}}{1-v_{pe}^2} z^2 dz = \int_{-h/2-t_{pe}}^{-h/2} \frac{v_{pe} E_{pe}}{1-v_{pe}^2} z^2 dz, \\
E_p &= \int_{h/2}^{h/2+t_{pe}} \frac{E_{pe}}{1-v_{pe}} \varepsilon_{pe} z dz = - \int_{-h/2-t_{pe}}^{-h/2} \frac{E_{pe}}{1-v_{pe}} \varepsilon_{pe} z dz, \\
\mathbb{G}_{pe} &= \int_{h/2}^{h/2+t_{pe}} 2G_{pe} l_{pe}^2 dz = \int_{-h/2-t_{pe}}^{-h/2} 2G_{pe} l_{pe}^2 dz.
\end{aligned}$$

Substituting Eqs. (6.3), (6.4) and (6.6) into (6.1), the differential governing equation of the composite laminated plate induced by two piezoelectric actuators can be derived as:

$$\begin{aligned}
(6.8) \quad & (\bar{I}_{11} + l^2 \tilde{Q}_{55}) \frac{\partial^4 w}{\partial x^4} + (2\bar{I}_{12} + 4\bar{I}_{66} + l^2 \tilde{Q}_{44} + l^2 \tilde{Q}_{55}) \frac{\partial^4 w}{\partial x^2 \partial y^2} + (\bar{I}_{22} + l^2 \tilde{Q}_{44}) \frac{\partial^4 w}{\partial y^4} \\
& + \left((2C_{11}^{12} + \mathbb{G}_{pe}) \frac{\partial^4 w}{\partial x^4} + (4C_{12}^{12} + 8C_{11}^{12} + 2\mathbb{G}_{pe}) \frac{\partial^4 w}{\partial x^2 \partial y^2} + (2C_{11}^{12} + \mathbb{G}_{pe}) \frac{\partial^4 w}{\partial y^4} \right) g(x, y) \\
& + 2E_p g_{xx} + 2E_p g_{yy} = 0
\end{aligned}$$

with

$$(6.9) \quad g(x, y) = [H(x - x_1) - H(x - x_2)][H(y - y_1) - H(y - y_2)],$$

$$(6.10) \quad \begin{aligned} g_{xx} &= [\delta'(x - x_1) - \delta'(x - x_2)][H(y - y_1) - H(y - y_2)], \\ g_{yy} &= [H(x - x_1) - H(x - x_2)][\delta'(y - y_1) - \delta'(y - y_2)]. \end{aligned}$$

In addition, the mechanical boundary conditions for a simply supported composite laminated plate and piezoelectric element can also be derived by the variational principle as:

$$(6.11) \quad \begin{aligned} w &= 0 \quad \text{at } x = 0 \text{ and } x = a, \\ w &= 0 \quad \text{at } y = 0 \text{ and } y = b. \end{aligned}$$

Introducing Eqs. (6.3), (6.4) and (6.6) into Hamilton's principle, the equations of motion of a rectangular micro-plate can be obtained as follows:

$$(6.12) \quad \begin{aligned} & - \frac{\partial^2(M_{cx} + Y_{cyx})}{\partial x^2} + \frac{\partial^2(-M_{cy} + Y_{cxy})}{\partial y^2} + \frac{\partial^2(-2M_{cxy} + Y_{cx} - Y_{cy})}{\partial x \partial y} \\ & + \left(\frac{\partial^2 \bar{M}_{xx}}{\partial x^2} + \frac{\partial^2 \bar{M}_{yy}}{\partial y^2} + \frac{\partial^2 \bar{M}_{xy}}{\partial x \partial y} \right) g(x, y) + 2E_p g_{xx}(x, y) + 2E_p g_{yy}(x, y) = 0. \end{aligned}$$

Also the corresponding boundary conditions are

$$\delta w = 0$$

or

$$(6.13) \quad \begin{aligned} & \frac{\partial(M_{cx} + Y_{cyx})}{\partial x} n_x - \frac{\partial(-M_{cy} + Y_{cxy})}{\partial y} n_y - \frac{1}{2} \frac{\partial(-2M_{cxy} + Y_{cx} - Y_{cy})}{\partial x} n_y n_y \\ & - \left[\frac{\partial(\bar{M}_{xx} + 2E_p)}{\partial x} n_x + \frac{\partial(\bar{M}_{yy} + 2E_p)}{\partial y} n_y + \frac{1}{2} \left(\frac{\partial \bar{M}_{xy}}{\partial x} n_y + \frac{\partial \bar{M}_{xy}}{\partial y} n_x \right) \right] g(x, y) \\ & - \frac{1}{2} \frac{\partial(-2M_{cxy} + Y_{cx} - Y_{cy})}{\partial y} n_x + 2E_p [n_x g_x(x, y) + n_y g_y(x, y)] = 0; \end{aligned}$$

$$\frac{\partial \delta w}{\partial x} = 0$$

or

$$\begin{aligned} & (-M_{cx} - Y_{cyx}) n_x + \frac{1}{2} (-2M_{cxy} + Y_{cx} - Y_{cy}) n_y \\ & + \left[(\bar{M}_{xx} + 2E_p) n_x + \frac{1}{2} \bar{M}_{xy} n_y \right] g(x, y) = 0, \end{aligned}$$

$$\frac{\partial \delta w}{\partial x} = 0$$

or

$$\begin{aligned} (-M_{cy} + Y_{cxy})n_y + \frac{1}{2}(-2M_{cxy} + Y_{cx} - Y_{cy})n_x + [(\bar{M}_{yy} + 2E_p)n_y \\ + \frac{1}{2}\bar{M}_{xy}n_x]g(x, y) = 0, \end{aligned}$$

where n_x and n_y are the components of normal vector to the boundary of mid-plane.

7. The solution of equilibrium equation

To the best of author's knowledge, the analytical solution of Eq. (6.8) is very difficult to obtain. In order to investigate how the size effect influences the deflection of the composite laminated plate and piezoelectric element, the the Ritz method [52] is used to derive the approximate solution of Eq. (6.8), in which the weak form of the variational statement of Eq. (6.8) is expressed as:

$$(7.1) \quad \iint \left\{ \begin{aligned} &(\bar{I}_{11} + l^2 \tilde{Q}_{55}) \frac{\partial^2 w}{\partial x^2} \frac{\partial^2 (\delta w)}{\partial x^2} + \bar{I}_{12} \left(\frac{\partial^2 w}{\partial x^2} \frac{\partial^2 (\delta w)}{\partial y^2} + \frac{\partial^2 w}{\partial y^2} \frac{\partial^2 (\delta w)}{\partial x^2} \right) \\ &+ (4\bar{I}_{66} + l^2 \tilde{Q}_{44}^+ l^2 \tilde{Q}_{55}) \frac{\partial^2 w}{\partial x \partial y} \frac{\partial^2 (\delta w)}{\partial x \partial y} + (\bar{I}_{22} + l^2 \tilde{Q}_{44}) \frac{\partial^2 w}{\partial y^2} \frac{\partial^2 (\delta w)}{\partial y^2} \\ &+ (2C_{11}^{12} + \mathbb{G}_{pe})g(x, y) \frac{\partial^2 w}{\partial x^2} \frac{\partial^2 (\delta w)}{\partial x^2} + 2C_{12}^{12} \left(\frac{\partial^2 w}{\partial x^2} \frac{\partial^2 (\delta w)}{\partial y^2} + \frac{\partial^2 w}{\partial y^2} \frac{\partial^2 (\delta w)}{\partial x^2} \right) \\ &+ (8C_{11}^{12} + 2\mathbb{G}_{pe})g(x, y) \frac{\partial^2 w}{\partial x \partial y} \frac{\partial^2 (\delta w)}{\partial x \partial y} + (2C_{11}^{12} + \mathbb{G}_{pe})g(x, y) \frac{\partial^2 w}{\partial y^2} \frac{\partial^2 (\delta w)}{\partial y^2} \\ &- (-2E_p g_{xx} - 2E_p g_{yy})(\delta w) \end{aligned} \right\} dx dy = 0.$$

The displacement w is assumed to be as following [52]:

$$(7.2) \quad w(x, y) \approx \sum_{i=1}^m \sum_{j=1}^n A_{ij} X_i(x) Y_j(y),$$

where A_{ij} are unknown constants to be determined, $X_i(x)$ and $Y_j(y)$ are coordinate functions which should satisfy the mechanical boundary conditions of plate. Thus for the simply support plate, $X_i(x)$ and $Y_j(y)$ are chosen as [52]:

$$(7.3) \quad X_i(x) = \sin \frac{i\pi x}{a}, \quad Y_j(y) = \sin \frac{j\pi y}{b}.$$

Substituting Eqs. (7.2) and (7.3) into Eq. (7.1), Eq. (7.1) can be reformulated as:

$$(7.4) \quad [R]\{A\} = \{F\}$$

with

$$(7.5) \quad R_{(ij)(kl)} = \iint \left[\begin{aligned} & (\bar{I}_{11} + l^2 \tilde{Q}_{55}) \frac{\partial^2 X_i}{\partial x^2} Y_j \frac{\partial^2 X_k}{\partial x^2} Y_l + \bar{I}_{12} \left(\frac{\partial^2 X_i}{\partial x^2} Y_j \frac{\partial^2 Y_l}{\partial y^2} X_k + \frac{\partial^2 Y_j}{\partial y^2} X_i \frac{\partial^2 X_k}{\partial x^2} Y_l \right) \\ & + (4\bar{I}_{66} + l^2 \tilde{Q}_{44}^+ l^2 \tilde{Q}_{55}) \frac{\partial X_i}{\partial x} \frac{\partial Y_j}{\partial y} \frac{\partial X_k}{\partial x} \frac{\partial Y_l}{\partial y} + (\bar{I}_{22} + l^2 \tilde{Q}_{44}) \frac{\partial^2 Y_j}{\partial y^2} X_i \frac{\partial^2 Y_l}{\partial y^2} X_k \\ & + (2C_{11}^{12} + G_{pe}) g(x, y) \frac{\partial^2 X_i}{\partial x^2} Y_j \frac{\partial^2 X_k}{\partial x^2} Y_l + 2C_{12}^{12} \left(\frac{\partial^2 X_i}{\partial x^2} Y_j \frac{\partial^2 Y_l}{\partial y^2} X_k + \frac{\partial^2 Y_j}{\partial y^2} X_i \frac{\partial^2 X_k}{\partial x^2} Y_l \right) \\ & + (8C_{11}^{12} + 2G_{pe}) g(x, y) \frac{\partial X_i}{\partial x} \frac{\partial Y_j}{\partial y} \frac{\partial X_k}{\partial x} \frac{\partial Y_l}{\partial y} + (2C_{11}^{12} + G_{pe}) g(x, y) \frac{\partial^2 Y_j}{\partial y^2} X_i \frac{\partial^2 Y_l}{\partial y^2} X_k \end{aligned} \right] dx dy$$

and

$$(7.6) \quad F_{kl} = \iint (-2E_1 g_{xx} - 2E_1 g_{yy}) X_k Y_l dx dy.$$

By solving the linear algebraic Eq. (7.4), the unknown constants A_{ij} are able to be obtained. Substituting the results of A_{ij} into Eq. (7.2), the deflection of the composite laminated plate and piezoelectric elements can be determined.

8. Numerical validation and examples

8.1. Verification studies

So far, there is no open literature on the research of size-dependent static bending of a cross-ply composite plate laminated with PZT actuators. In order to verify the model proposed in this paper, a classical static bending of a cross-ply laminated plate composed of carbon/epoxy with stacking sequence [0/90/90/0] is firstly considered. The sizes of the composite laminated plate model: length of the plate is $a = 0.38$ m, width is $b = 0.3$ m and thickness is $h = 1.5876$ mm. As depicted in Fig. 2, a pair of PZT G-1195 actuators is symmetrically pasted on the upper and lower surface of the composite plate, respectively. The top and bottom actuators are subjected to voltages of +1 V and -1 V, respectively.

Table 1 and Table 2 list properties of carbon/epoxy and PZT G-1195, respectively. The sizes of piezoelectric actuators are assumed to be $0.06 \text{ m} \times 0.04 \text{ m}$, $0.08 \text{ m} \times 0.06 \text{ m}$ and $0.10 \text{ m} \times 0.08 \text{ m}$, respectively. The thickness of piezoelectric actuator t_{pe} is set to be $0.1h$, $0.4h$, $0.8h$ and h , respectively.

Table 3 lists the induced central deformation of this plate with three different geometric dimensions and constant thickness ($t_{pe} = 0.1h$) by using a finite element code written in FORTRAN90 programming language at the Nanjing University of Aeronautics and Astronautics [53, 54], the Ritz method and ANSYS. The comparison presented in Table 3 show that the results derived by the Ritz

Table 1. Material properties of carbon/epoxy.

Longitudinal modulus E_1	Transverse modulus E_2	Shear modulus G_{12}	Shear modulus G_{23}	Poisson's ratio ν_{12}	Poisson's ratio ν_{23}
108 Gpa	10.3 Gpa	7.13 Gpa	4.02 Gpa	0.28	0.28

Table 2. Material properties of PZT G-1195.

Young's modulus E_{pe}	Poisson's ratio ν_{pe}	density ρ_{pe}	Piezoelectric constant d_{31}
63 Gpa	0.3	7600 kg/m ²	1.9×10^{-10} V/m

Table 3. Maximum deflection of the composite plate induced by the piezoelectric actuators with three different sizes and constant thickness ($t_{pe} = 0.1h$).

Size	ANSYS	FEM	Ritz
0.06 m \times 0.04 m	1.170×10^{-6} m	1.197×10^{-6} m	1.208×10^{-6} m
0.08 m \times 0.06 m	2.050×10^{-6} m	2.076×10^{-6} m	2.087×10^{-6} m
0.10 m \times 0.08 m	3.030×10^{-6} m	3.049×10^{-6} m	3.054×10^{-6} m

method matches well with those of the finite element method (FEM) [53, 54] and ANSYS. This comparison also verifies the correctness of the household finite element code.

Table 4 lists the induced central deformation of this plate with four different thicknesses and constant size (0.08 m \times 0.06 m) of the equivalent bending moment model proposed in Section 5 and refined model developed in Section 6. By comparing the results obtained through FEM with outcome given by two models presented in this paper, we can find the differences of two models are negligible when the thickness of piezoelectric actuators is far less than that of the composite laminated plate. And the bending moment model cannot describe the deflection quite well if the thicknesses of piezoelectric actuator and composite laminated plates are close to each other. Hence, we only present the results of the refined model in the following size-dependent analysis.

Table 4. Maximum deflection of the composite plate induced by the piezoelectric actuators with four different thicknesses and constant size (0.08 m \times 0.06 m).

t_{pe}/h	Bending moment model	Refined model	FEM
0.1	1.894×10^{-6} m	2.087×10^{-6} m	2.076×10^{-6} m
0.4	0.7095×10^{-6} m	0.8131×10^{-6} m	0.7888×10^{-6} m
0.8	0.3089×10^{-6} m	0.3783×10^{-6} m	0.3674×10^{-6} m
1	0.2244×10^{-6} m	0.2806×10^{-6} m	0.2734×10^{-6} m

8.2. Numerical examples

After verification of the present size-dependent plate model, the size-dependent static bending analysis of a simply supported laminated cross-ply plate is illustrated. Consider a four-layer $[0^\circ/90^\circ/90^\circ/0^\circ]$ laminated plate with the size of length $a = 380 \mu\text{m}$, width $b = 300 \mu\text{m}$ thickness $h = 40 \mu\text{m}$. The material constants [55]: $E_2 = 6.98 \text{ GPa}$, $E_1 = 25E_2$, $G_{12} = 0.5E_2$, $\nu_{12} = \nu_{22} = 0.25$, $\nu_{21}^k = E_2^k \nu_{12}^k / E_1^k$. The top and bottom PZT actuators are subjected to voltages of $+1 \text{ V}$ and -1 V , respectively.

For piezoelectric actuator, the material length scale parameter l_{pe} is assumed to be equal to the values of micro-material's constants of composite laminated plate ($l_{pe} = l_{kb} = l$) [36, 56].

Figure 3 shows the normalized transverse displacement in the line of $y = b/2$ and the line of $x = a/2$ of the composite laminated plate. Piezoelectric actuators,

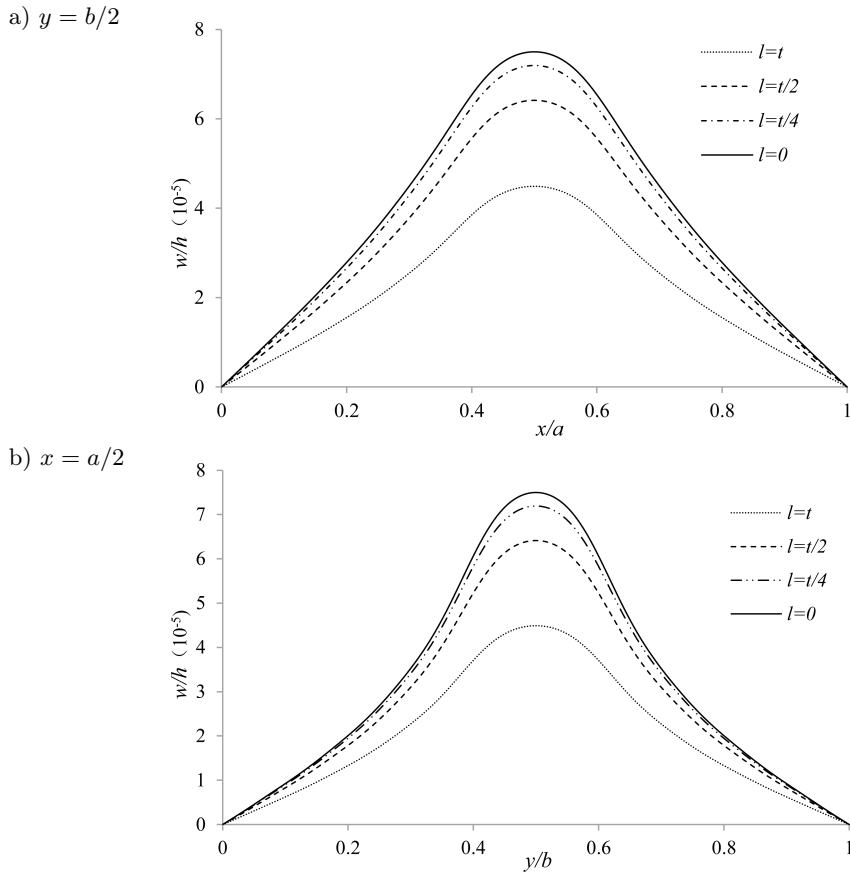


FIG. 3. Variations of normalized transverse displacement of composite laminated plate, w/h , for different material length scale parameters ($80 \times 60 \mu\text{m}$, $t_{pe}/h = 0.1$).

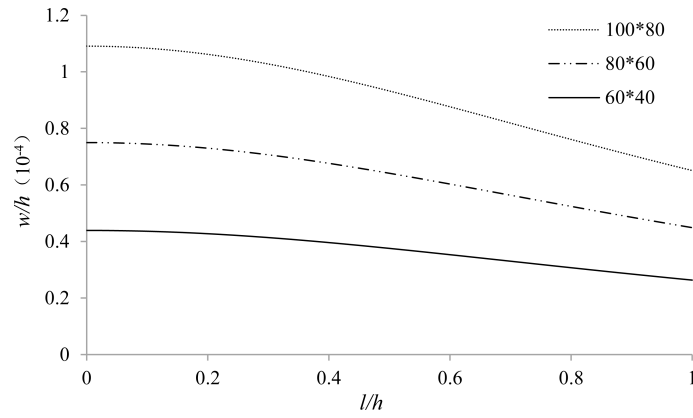
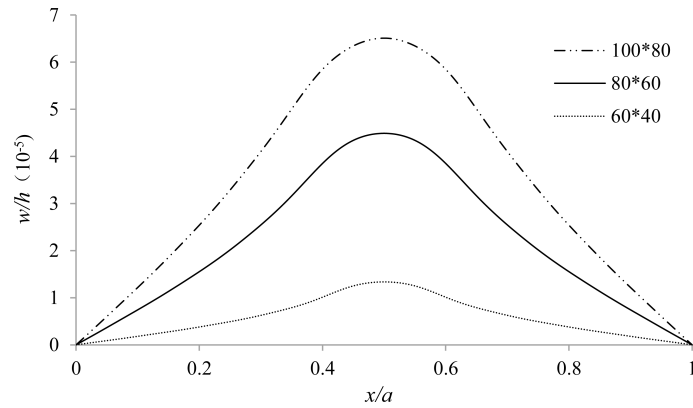


FIG. 4. Effect of the dimensionless material length scale parameters on normalized maximum deflection of composite laminated plate ($t_{pe}/h = 0.1$).

a) $y = b/2$



b) $x = a/2$

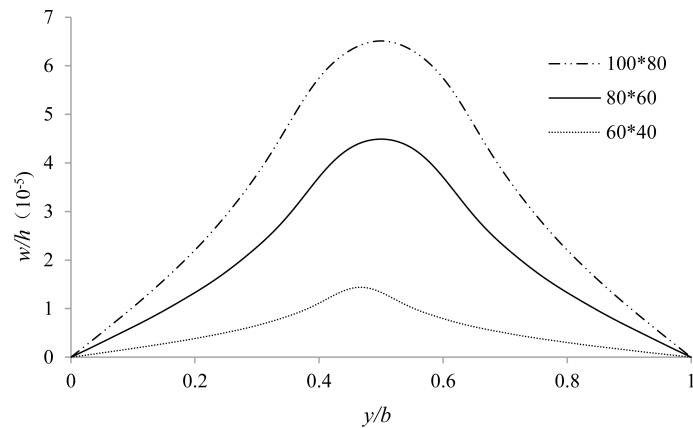


FIG. 5. Variations of normalized transverse displacement of composite laminated plate, w/h , for different sizes of piezoelectric actuators ($l = h$, $t_{pe}/h = 0.1$).

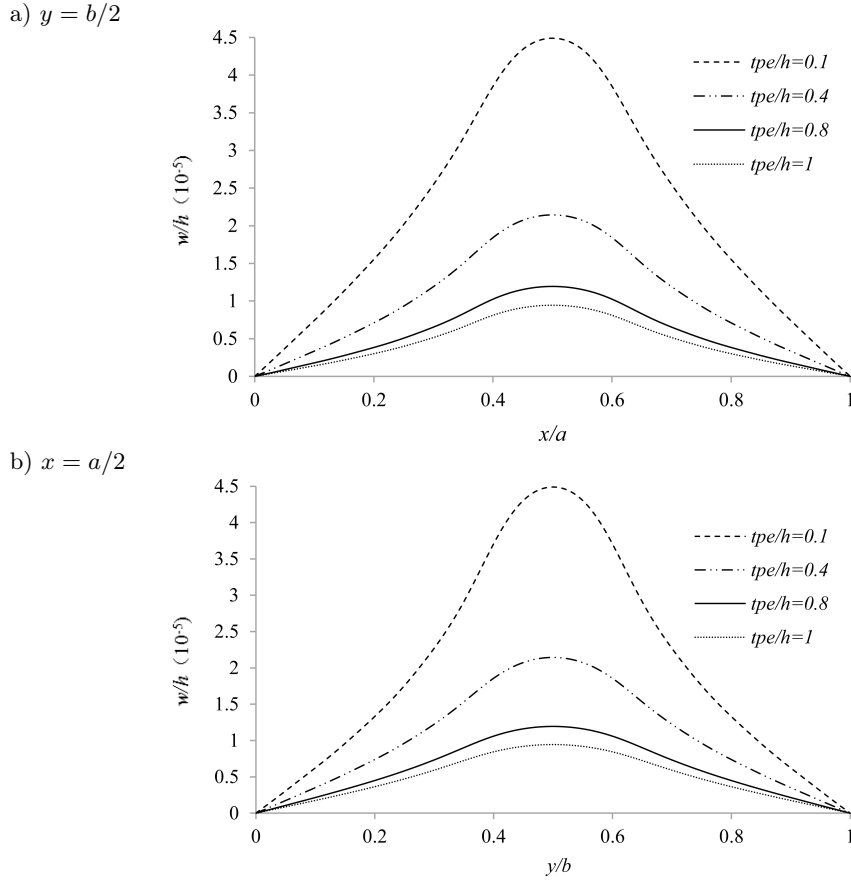


FIG. 6. Variations of normalized transverse displacement of composite laminated plate, w/h , for different thicknesses of piezoelectric actuators ($l = h$, $80 \times 60 \mu\text{m}$).

with the dimension of $80 \times 60 \mu\text{m}$, pasted at the center of the aforementioned plate symmetrically. Figure 4 illustrates the normalized maximum deflection variations of composite laminated plate in terms of the dimensionless material length scale parameters for different sizes of piezoelectric actuators ($100 \times 80 \mu\text{m}$, $80 \times 60 \mu\text{m}$, $60 \times 40 \mu\text{m}$) and constant thickness of piezoelectric actuators ($t_{pe}/h = 0.1$). These two figures demonstrate that the normalized maximum deflections decrease with increasing MLSP. Furthermore, the closer the position is to the central area, the larger the deflection, and the smaller the material length scale parameter, the larger the increasing rate of the deflection. Figure 4 also shows the effect of l on the decreasing rates of the normalized maximum deflections becomes more significant when the size of the actuator is larger.

Numerical results demonstrate that the size-dependent deformations of the composite micro-plate are smaller than classical ones ($l/h = 0$). This means

the size effect should be considered as the size of the structure scales down to micrometers. Apparently, the composite laminated plate stiffens as the material length scale parameter increases.

Figure 5 presents the normalized transverse deflection in the line of $y = b/2$ and the line of $x = a/2$ of the composite laminated plate for constant thickness of piezoelectric actuators, material length scale parameter ($l = h$, $t_{pe}/h = 0.1$) and different sizes of piezoelectric actuators ($100 \times 80 \mu\text{m}$, $80 \times 60 \mu\text{m}$, $60 \times 40 \mu\text{m}$). Obviously, normalized transverse displacement increases with the increasing size of an actuator.

Figure 6 plots the normalized transverse deflection in the line of $y = b/2$ and the line of $x = a/2$ of the composite laminated plate for constant size of piezoelectric actuator ($80 \times 60 \mu\text{m}$) material length scale parameter ($l = h$) and various thickness of piezoelectric actuator ($t_{pe}/h = 0.1$, $t_{pe}/h = 0.4$, $t_{pe}/h = 0.8$, $t_{pe}/h = 1.0$). Figure 7 indicates the influence of the dimensionless thickness of piezoelectric actuators on the normalized maximum deformation of composite laminated plate for different sizes of piezoelectric actuators ($100 \times 80 \mu\text{m}$, $80 \times 60 \mu\text{m}$, $60 \times 40 \mu\text{m}$) and the constant material length scale parameter ($l = h$). Figure 6 and Figure 7 show that the normalized maximum deflections increase with the decrease in an actuator thickness. This means that the increase in the actuator thickness seems to have a greater impact on the bending rigidity of the plate than it does on driving forces. Figure 7 also shows that the decreasing rates of the normalized maximum deflections increase with increasing actuator sizes. In addition, the lesser the actuator thickness, the faster the decreasing rates of maximum deformations. The decreasing rates of normalized maximum deformations have a descending trend with respect to an actuator thickness and vice versa.

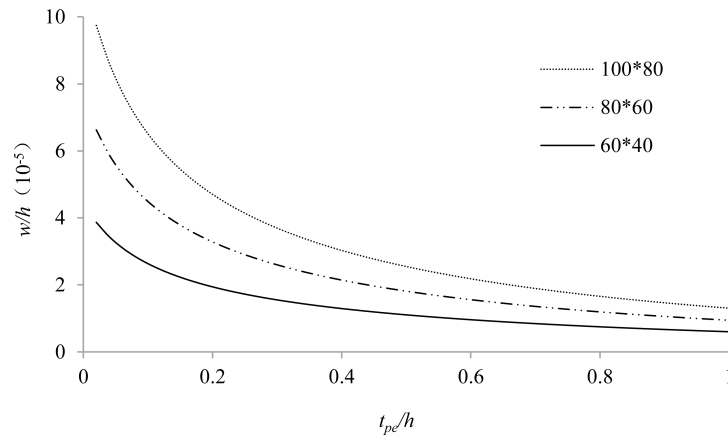


FIG. 7. Effect of the dimensionless thickness of piezoelectric actuators on normalized maximum deflection of composite laminated plate ($l = h$).

9. Discussion and conclusions

By using the RMCST, this paper presents a size-dependent analysis for the transverse deformation of the cross-ply composite laminated plate bonded with PZT actuators for the first time. Equal-amplitude voltages with an opposite sign are acted to the top and bottom piezoelectric actuators. The Ritz approximate solution of deflection indicates that the size-effect cannot be ignored in micro-scale. Numerical examples illustrate that the size-dependent deflection of composite laminated plate are strongly dependent on the material length scale parameter and the dimension of piezoelectric actuators. These discussions suggest the following conclusions:

(1) For thinner piezoelectric actuators, the results of the model using equivalent bending moments correlate well with those of the Ritz method. But when the ratio of actuator thickness to host beam thickness becomes larger, the results of the model using equivalent bending moments seem to be significantly lesser in comparison with corresponding values computed by the Ritz method and FEA.

(2) The influence of MLSP on the decreasing rates of the normalized maximum deflections becomes more significant when the size of the actuator is larger.

(3) The lesser the actuator thickness, the faster the decreasing rates of normalized maximum deformations. The decreasing rates of normalized maximum deformations have a descending trend with respect to increasing actuator thickness and an increasing trend with the increasing length and width of the PZT actuator.

(4) Because of the difficulty of experiments at micro scale and time consuming of MD (molecular dynamics) calibration [57], researchers generally study the variations of size-dependent performances versus assumed material length scale parameters. For piezoelectric based laminated structures, the material length scale parameters of piezoelectric layer are usually assumed to be zero [58, 59] or equal to that of substrate [35, 36, 56]. The approach of determining MLSP will remain to be continued to improve authors' future works.

Declaration of conflicting interests

The author(s) declared no potential conflicts of interest with respect to the research, authorship, and/or publication of this article.

Acknowledgement

This research was partially supported by the National Natural Science Foundation of China (grant No. 11572151), the Priority Academic Program Development of Jiangsu Higher Education Institutions. The authors are very grateful for the financial support.

References

1. S.C. HER, C.S. LIN, *Deflection of cross-ply composite laminates induced by piezoelectric actuators*, *Sensors*, **10**, 719–733, 2010.
2. E.F. CRAWLEY, J. DE LUIS, *Use of piezoelectric actuators as elements of intelligent structures*, *AIAA Journal*, **25**, 1373–1385, 1987.
3. G.L. HUANG, C.T. SUN, *The dynamic behaviour of a piezoelectric actuator bonded to an anisotropic elastic medium*, *International Journal of Solids and Structures*, **43**, 1291–1307, 2006.
4. E. DIMITRIADIS, C. FULLER, C. ROGERS, *Piezoelectric actuators for distributed vibration excitation of thin plates*, *Journal of Vibration and Acoustics*, **113**, 100–107, 1991.
5. Q. LUO, L. TONG, *High precision shape control of plates using orthotropic piezoelectric actuators*, *Finite Elements in Analysis and Design*, **42**, 1009–1020, 2006.
6. J.-C. LIN, M. NIEN, *Adaptive modeling and shape control of laminated plates using piezoelectric actuators*, *Journal of Materials Processing Technology*, **189**, 231–236, 2007.
7. C. BOWEN, R. BUTLER, R. JERVIS, H. KIM, A. SALO, *Morphing and shape control using unsymmetrical composites*, *Journal of Intelligent Material Systems and Structures*, **18**, 89–98, 2007.
8. P. GIDDINGS, C. BOWEN, R. BUTLER, H. KIM, *Characterisation of actuation properties of piezoelectric bi-stable carbon-fibre laminates*, *Composites Part A: Applied Science and Manufacturing*, **39**, 697–703, 2008.
9. J.Y. PARK, Y.J. YEE, H.J. NAM, J.U. BU, [in:] *Microwave Symposium Digest, 2001 IEEE MTT-S International*. (IEEE, 2001), vol. 3, pp. 2111–2114.
10. S. TADIGADAPA, K. MATETI, *Piezoelectric MEMS sensors: state-of-the-art and perspectives*, *Measurement Science and Technology*, **20**, 092001, 2009.
11. N. FLECK, G. MULLER, M. ASHBY, J. HUTCHINSON, *Strain gradient plasticity: theory and experiment*, *Acta Metallurgica et Materialia*, **42**, 475–487, 1994.
12. D. LAM, F. YANG, A. CHONG, J. WANG, P. TONG, *Experiments and theory in strain gradient elasticity*, *Journal of the Mechanics and Physics of Solids*, **51**, 1477–1508, 2003.
13. R. MINDLIN, H. TIERSTEN, *Effects of couple-stresses in linear elasticity*, *Archive for Rational Mechanics and Analysis*, **11**, 415–448, 1962.
14. R.A. TOUPIN, *Elastic materials with couple-stresses*, *Archive for Rational Mechanics and Analysis*, **11**, 385–414, 1962.
15. A.C. ERINGEN, *Nonlocal polar elastic continua*, *International Journal of Engineering Science*, **10**, 1–16, 1972.
16. F. YANG, A. CHONG, D. LAM, P. TONG, *Couple stress based strain gradient theory for elasticity*, *International Journal of Solids and Structures*, **39**, 2731–2743, 2002.
17. S. PARK, X. GAO, *Bernoulli–Euler beam model based on a modified couple stress theory*, *Journal of Micromechanics and Microengineering*, **16**, 2355, 2006.
18. S. KONG, S. ZHOU, Z. NIE, K. WANG, *The size-dependent natural frequency of Bernoulli–Euler micro-beams*, *International Journal of Engineering Science*, **46**, 427–437, 2008.

19. M. KAHROBAIYAN, M. ASGHARI, M. RAHAEIFARD, M. AHMADIAN, *Investigation of the size-dependent dynamic characteristics of atomic force microscope microcantilevers based on the modified couple stress theory*, International Journal of Engineering Science, **48**, 1985–1994, 2010.
20. H.M. MA, X.L. GAO, J.N. REDDY, *A microstructure-dependent Timoshenko beam model based on a modified couple stress theory*, Journal of the Mechanics and Physics of Solids, **56**, 3379–3391, 2008.
21. L.L. KE, Y.S. WANG, *Flow-induced vibration and instability of embedded double-walled carbon nanotubes based on a modified couple stress theory*, Physica E: Low-dimensional Systems and Nanostructures, **43**, 1031–1039, 2011.
22. Y. FU, J. ZHANG, *Modeling and analysis of microtubules based on a modified couple stress theory*, Physica E: Low-dimensional Systems and Nanostructures, **42**, 1741–1745, 2010.
23. H.M. MA, X.-L. GAO, J.N. REDDY, *a nonclassical Reddy-Levinson beam model based on a modified couple stress theory*, International Journal for Multiscale Computational Engineering, **8**, 167–180, 2010.
24. G.C. TSIATAS, *A new Kirchhoff plate model based on a modified couple stress theory*, International Journal of Solids and Structures, **46**, 2757–2764, 2009.
25. J. ABDI, A. KOOCHI, A. KAZEMI, M. ABADYAN, *Modeling the effects of size dependence and dispersion forces on the pull-in instability of electrostatic cantilever NEMS using modified couple stress theory*, Smart Materials and Structures, **20**, 055011, 2011.
26. Y.T. BENI, A. KOOCHI, M. ABADYAN, *Theoretical study of the effect of Casimir force, elastic boundary conditions and size dependency on the pull-in instability of beam-type NEMS*, Physica E: Low-dimensional Systems and Nanostructures, **43**, 979–988, 2011.
27. M. KOMIJANI, J.N. REDDY, A.J.M FERREIRA, *Nonlinear stability and vibration of pre/post-buckled microstructure-dependent FGPM actuators*, Meccanica, **49**, 2729–2745, 2014.
28. Y.S. LI, W.J. FENG, Z.Y. CAI, *Bending and free vibration of functionally graded piezoelectric beam based on modified strain gradient theory*, Composite Structures, **115**, 41–50, 2014.
29. A.A. JANDAGHIAN, O. RAHMANI, *Size-dependent free vibration analysis of functionally graded piezoelectric plate subjected to thermo-electro-mechanical loading*, Journal of Intelligent Material Systems and Structures, **28**, 3039–3053, 2017.
30. Y.S. LI, E. PAN, *Static bending and free vibration of a functionally graded piezoelectric microplate based on the modified couple-stress theory*, International Journal of Engineering Science, **97**, 40–59, 2015.
31. R. ANSARI, M.A. ASHRAFI, S. HOSSEINZADEH, *Vibration Characteristics of Piezoelectric Microbeams Based on the Modified Couple Stress Theory*, Shock and Vibration, **2014**, 598292-1-12, 2014.
32. A.G. ARANI, M. ABDOLLAHIAN, R. KOLAHCHI, *Nonlinear vibration of a nanobeam elastically bonded with a piezoelectric nanobeam via strain gradient theory*, International Journal of Mechanical Science, **100**, 32–40, 2015.
33. A. ABDOLLAHI, C. PECO, D. MILLÁN, M. ARROYO, I. ARIAS, *Computational evaluation of the flexoelectric effect in dielectric solids*, Journal of Applied Physics, **116**, 093502, 2014.

34. Z. YAN, L.Y. JIANG, *Flexoelectric effect on the electroelastic responses of bending piezoelectric nanobeams*, Journal of Applied Physics, **113**, 194102-194102-194109, 2013.
35. S. ZHENG, M. CHEN, Z. LI, H. WANG, *Size-dependent constituent equations of piezoelectric bimorphs*, Composite Structures, **150**, 1–7, 2016.
36. M. CHEN, S. ZHENG, *Size-dependent static bending of a micro-beam with a surface-mounted 0–1 polarized PbLaZrTi actuator under various boundary conditions*, Journal of Intelligent Material Systems and Structures, **28**, 2920–2932, 2017.
37. M. AREFI, A.M. ZENKOUR, *Vibration and bending analysis of a sandwich microbeam with two integrated piezo-magnetic face-sheets*, Composite Structures, 2016.
38. M. AREFI, A.M. ZENKOUR, *Transient analysis of a three-layer microbeam subjected to electric potential*, International Journal of Smart and Nano Materials, **8**, 20–40, 2017.
39. S. SAHMANI, M. BAHRAMI, *Size-dependent dynamic stability analysis of microbeams actuated by piezoelectric voltage based on strain gradient elasticity theory*, Journal of Mechanical Science and Technology, **29**, 325–333, 2015.
40. A. LI, S. ZHOU, S. ZHOU, B. WANG, *Size-dependent analysis of a three-layer microbeam including electromechanical coupling*, Composite Structures, **116**, 120–127, 2014.
41. W.J. CHEN, M. XU, L. LI, *A model of composite laminated Reddy plate based on new modified couple stress theory*, Composite Structures, **94**, 2143–2156, 2012.
42. W.J. CHEN, X.P. LI, *Size-dependent free vibration analysis of composite laminated Timoshenko beam based on new modified couple stress theory*, Archive of Applied Mechanics, **83**, 431–444, 2013.
43. W. CHEN, Y. WANG, *A model of composite laminated Reddy plate of the global-local theory based on new modified couple-stress theory*, Mechanics of Advanced Materials and Structures, **23**, 636–651, 2016.
44. M. MOHAMMADABADI, A. DANESHMEHR, M. HOMAYOUNFARD, *Size-dependent thermal buckling analysis of micro composite laminated beams using modified couple stress theory*, International Journal of Engineering Science, **92**, 47–62, 2015.
45. CH. WANJI, W. CHEN, K.Y. SZE, *A model of composite laminated Reddy beam based on a modified couple-stress theory*, Composite Structures, **94**, 2599–2609, 2012.
46. H.A.C. TILMANS, R. LEGTENBERG, *Electrostatically driven vacuum-encapsulated polysilicon resonators: Part II. Theory and performance*, Sensors and Actuators A: Physical, **45**, 67–84, 1994.
47. R.C. BATRA, M. PORFIRI, D. SPINELLO, *Review of modeling electrostatically actuated microelectromechanical systems*, Smart Materials and Structures, **16**, R23-R31, 2007.
48. M. RUAN, J. SHEN, C.B. WHEELER, *Latching microelectromagnetic relays*, Sensors and Actuators A: Physical, **91**, 346–350, 2001.
49. G. REZAZADEH, F. KHATAMI, A. TAHMASEBI, *Investigation of the torsion and bending effects on static stability of electrostatic torsional micromirrors*, Microsystem Technologies, **13**, 715–722, 2007.
50. M.H. KORAYEM, A. HOMAYOONI, *The size-dependent analysis of multilayer micro-cantilever plate with piezoelectric layer incorporated voltage effect based on a modified couple stress theory*, European Journal of Mechanics - A/Solids, **61**, 59–72, 2017.

51. G.M. REBEIZ, *RF MEMS: Theory, design, and technology*, Microwaves & Rf, 87–120, 2004.
52. J.N. REDDY, *Theory and Analysis of Elastic Plates and shells*, CRC Press, 2006.
53. S.J. ZHENG, F. DAI, Z. SONG, *Active control of piezothermoelastic FGM shells using integrated piezoelectric sensor/actuator layers*, International Journal of Applied Electromagnetics and Mechanics, **30**, 107–124, 2009.
54. S. ZHENG, L. TONG, Q. LUO, *Finite element formulations and algorithms for coupled multiphysics analysis of 0-1 and 0-3 polarized PLZT actuators*, International Journal of Applied Electromagnetics and Mechanics, **49**, 513–530, 2015.
55. N.J. PAGANO, *Exact solutions for rectangular bidirectional composites and sandwich plates*, Journal of Composite Materials, **4**, 20–34, 1970.
56. S. ZHENG, Z. LI, M. CHEN, H. WANG, *Size-dependent static bending and free vibration of 0–3 polarized PLZT microcantilevers*, Smart Materials and Structures, **25**, 085025, 2016.
57. F. MEHRALIAN, Y. TADI BENI, M. KARIMI ZEVEERDEJANI, *Calibration of nonlocal strain gradient shell model for buckling analysis of nanotubes using molecular dynamics simulations*, Physica B: Condensed Matter, **521**, 102–111, 2017.
58. Y. XIAO, B.L. WANG, S.J. ZHOU, *Pull-in voltage analysis of electrostatically actuated MEMS with piezoelectric layers: a size-dependent model*, Mechanics Research Communications, **66**, 7–14, 2015.
59. J.B. SHEN, H.T. WANG, S.J. ZHENG, *Size-dependent pull-in analysis of a composite laminated micro-beam actuated by electrostatic and piezoelectric forces: generalized differential quadrature method*, International Journal of Mechanical Science, **135**, 353–361, 2018.

Received September 13, 2018; revised version April 10, 2019.

Published online June 28, 2019.
